All-Optical Switching Using a Hybrid Plasmonic Donut Resonator With Photothermal Absorber

Xu Sun, Xi Chen, Min Yan, Min Qiu, Lars Thylén, and Lech Wosinski

***Abstract*— A novel hybrid plasmonic (HP) donut resonator integrated with a photothermal plasmonic absorber has been developed, which can be used as a compact all-optical switch or modulator. The radius of the fabricated HP donut resonator is 1.8 μm, with a resonant wavelength around 1550 nm and a quality factor (*Q* factor) around 600. The photothermal plasmonic absorber is directly integrated above the HP device, which can absorb as much as 75% of impinging optical power at 1064 nm wavelength. Since the absorber is in tight contact to the Si ridge of the HP waveguide, the absorbed optical power can efficiently heat up the Si ridge, and hence change the resonant wavelength of the HP donut resonator by Si thermal expansion effect. Experimental results show that the power used for 15 dB amplitude switch is only 10 mW, with rise and fall response times around 18 and 14 μs, respectively.**

***Index Terms*— Integrated optics, plasmons, optical resonators.**

I. INTRODUCTION

SILICON-ON-INSULATOR (SOI) on-chip photonic devices show the advantages of low propagation loss, high refractive index and CMOS compatible fabrication process, and therefore are considered as the most promising technology platform for realizing photonic integrated circuits (PICs) towards optical communication, bio-sensing, optical interconnect and data processing. However, the low Pockels electro-optic effect and indirect bandgap of Si material limit the development of SOI technology for active optical components, such as modulators and light sources. Moreover, the diffraction limited modal field of a Si waveguide also restricts further reduction of the size of SOI photonic devices. To overcome these limitations, other materials, such as semiconductor materials (Ge, GaAs, InP, etc), nonlinear crystals ($LiNO_3$, $LiTaO_3$, etc), organic materials (electro-optics polymers) and plasmonic materials (silver, gold and copper) have been extensively studied for their possible integration into SOI platform to increase functionalities of SOI devices, including sub-wavelength light guidance (using plasmonic materials) [1]–[4], light modulation [3], [5], [6] and lasing [7] (semiconductors or organic materials).

Hybrid Si-plasmonic (HP) waveguide [4], a combination of SOI photonics structure and surface plasmon polariton (SPP), can support subwavelength optical confinement with relative low propagation loss. In recent years, many HP waveguide structures have been designed and fabricated [1], [2], [8], which can realize various functions with compact size. For example, sub-wavelength waveguiding and coupling [1], [2], [9], [10], optical power splitting [11], polarization splitting [12], [13] and high-sensitivity refractive index sensing [8], [14]. Particularly, due to the large optical confinement, HP ring/disk resonators can offer better *Q* and Purcell factors compared to pure Si ones, when the radius is small (less than 1μm) [6], [15]. However, most proposed HP waveguide structures are either difficult to fabricate [1], [4] or not suitable for long range on-chip communication [2], which limit the development of such devices.

In this letter, we propose a novel SOI compatible HP waveguide structure, where only the active region is covered by plasmonic layer. The influence of plasmonic loss can be dramatically reduced in comparison to the one with metal underneath [2] (where plasmonic losses exist in the whole device). Moreover, the fabrication process is much easier compared to the HP waveguide with metal cap [1]. By integrating the plasmonic layer with metal-insulator-metal (MIM) photothermal absorber [16], we experimentally realize an all-optical switching HP donut resonator with a compact size.

II. SCHEMATIC

As shown in Figs. 1(a) and (b), the HP waveguide is composed of a Si ridge, thin SiO_2 layer and plasmonic material layer (Ag is used in this letter due to low plasmonic loss). Al_2O_3 is thermally evaporated beside the Si ridge in order to flatten the interface between Si ridge and SiO_2 layer. The photothermal plasmonic absorber, with Au-Al_2O_3-Au structure, is directly evaporated above the HP waveguide. One should notice that the lower Au layer of the photothermal absorber can also be replaced by the Ag layer of the HP waveguide with nearly no influence on optical properties,

Manuscript received March 16, 2016; revised April 20, 2016; accepted April 22, 2016. Date of publication April 28, 2016; date of current version May 23, 2016. This work was supported by the Swedish Research Council (VR) through its Linnæus Center of Excellence ADOPT. X. Sun acknowledges China Scholarship Council (CSC) for the financial support.

X. Sun and L. Wosinski are with the School of Information and Communication Technology, KTH Royal Institute of Technology, Kista 164 40, Sweden, and also with the Joint Research Center of Photonics of the Royal Institute of Technology (Sweden) and Zhejiang University (China) (JORCEP) (e-mail: xus@kth.se; lech@kth.se).

X. Chen and M. Yan are with the School of Information and Communication Technology, KTH Royal Institute of Technology, Kista 164 40, Sweden (e-mail: xc@kth.se; miya@kth.se).

M. Qiu is with the State Key Laboratory of Modern Optical Instrumentation, Zhejiang University, Hangzhou 310027, China (e-mail: minqiu@zju.edu.cn).

L. Thylén is with the School of Information and Communication Technology, KTH Royal Institute of Technology, Kista 164 40, Sweden, also with the Joint Research Center of Photonics of the Royal Institute of Technology (Sweden) and Zhejiang University (China) (JORCEP), and also with Hewlett-Packard Enterprise Laboratories, Palo Alto, CA 94304 USA (e-mail: lthylen@kth.se).

Color versions of one or more of the figures in this letter are available online at http://ieeexplore.ieee.org.

Digital Object Identifier 10.1109/LPT.2016.2558478

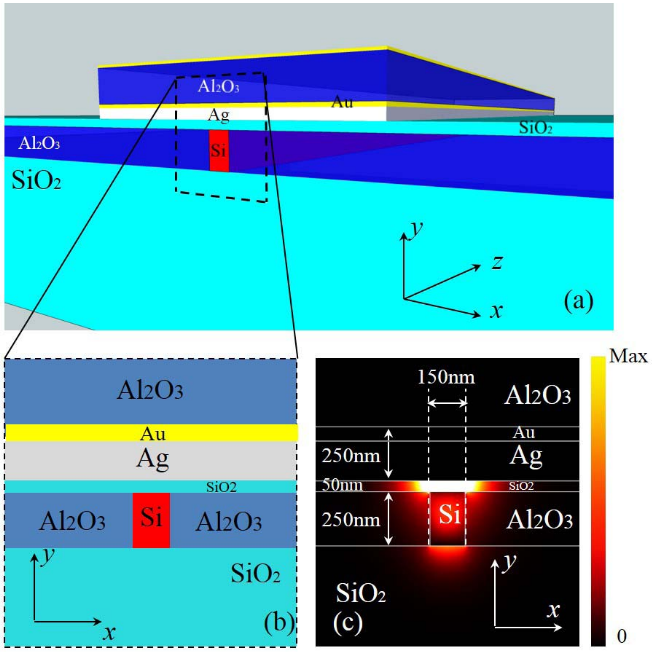

Fig. 1. (a) Schematic of an HP waveguide integrated with photothermal plasmonic absorber. (b) Cross-section view of HP waveguide. (c) Power distribution of TM mode supported by HP waveguide.

however, in our design, the lower Au layer is to protect the Ag layer underneath from oxidation in air during the fabrication processes.

Fig. 1(c) is the power distribution of the HP waveguide, where a transverse-magnetic (TM) polarization mode is supported. The optical parameters of the materials used for simulation are taken from [6] and [8]. As shown in the figure, the optical power is highly confined in the low-index SiO_2 layer, and can be propagated along the Si ridge with subwavelength size. As for the donut resonator, the width of the ring is wider than the width of the access waveguide to obtain high Q factor, similarly to a disk resonator, but maintaining single mode operation [15]. From simulation, an HP donut resonator with 450nm width Si ridge has an effective refractive index (n_{eff}) of 2.29, which is higher than the one of Si waveguide with similar size (in this case $n_{eff} = 1.957$). The large n_{eff} of HP waveguide is the reason for its low radiation loss at sharp bends [9], and hence gives a high Q factor of ring/disk resonators with small radius [6], [17]. Moreover, one can observe that a considerable part of optical power is confined in the Si ridge, which can be used for modulation functions using the large Si thermal expansion effect. Since the distance between the Si ridge and photothermal absorber is quite small (only several tens of nanometers), the heating efficiency is much higher compared to the photothermal devices based on SOI platform [18]–[20].

III. Experimental Realization

For the fabrication, a commercially available SOI wafer with 250nm crystalline Si on top and 3μm SiO_2 buffer was used. The first e-beam lithography (EBL) with negative resist was performed for patterning the structure of Si ridge. After that, inductively coupled plasma (ICP) dry etching was the next step. The etching depth was about 230nm, and the remaining 20nm Si material (not shown in Fig. 1) was used as a thermal conductivity layer due to the low thermal conductivity of the substrate material (SiO_2) (the thermal conductivities for SiO_2 and Si are 1.4W/mK and 142W/mK, respectively). Al_2O_3 material was e-beam evaporated after ICP etching process (the resist remaining), then metal lift-off was performed. The thickness of the evaporated Al_2O_3 layer was similar to the etching depth of the Si ridge ($\sim$230nm); in this way, the surface was flattened for further processes. Second EBL patterning with positive resist and ICP etching were applied to fabricate the grating couplers for light in-out coupling [21] at each end of the device. After removing the resist, plasma enhanced chemical vapor deposition (PECVD) was performed to add a thin SiO_2 layer ($\sim$50nm). Then, the third EBL patterning with positive resist was used to open the areas of plasmonic layer and photothermal absorber. E-beam evaporation and lift-off processes followed again to form the final optical component, as shown in the scanning electron microscope (SEM) images in Fig. 2. The mean radius of the HP donut was designed to be 1.8μm, since for this size, the absorption loss dominates over radiation loss, and hence the Q factor does not further increase with an increasing radius [6]. The radius of the photothermal plasmonic absorber is 10μm to collect enough optical power from the driving laser beam. In our experiment, the radius of the photothermal absorber is designed to match the size of single mode optical fiber connected to the driving laser. It can be further decreased when better focusing of the driving laser beam is implemented. The width of the Si bus waveguide (outside the absorber) is around 400nm, while the width of the Si ridge in the center active area (HP waveguide) is about 200nm. As one can notice from the upper right inset in Fig. 2, the tiny gaps between the Si ridge and the Al_2O_3 layer are formed due to the slope of the negative resist in the first EBL process, however, it does not influence the results noticeably. The cross-section view is shown in the lower left inset in Fig. 2, where the different material layers have been clearly illustrated.

For static characterization, a fiber connected to a tunable continuous wave (CW) laser (wavelength ranges from 1460nm to 1580nm) is located above the grating coupler at one end of the device. Polarization controller is used to select the proper mode (TM mode for HP waveguide). At the other end of the device, another optical fiber linked with an optical spectrum analyzer (OSA) is inserted above the second grating coupler to collect and show the transmitted power. For dynamic characterization, an InGaAs photodetector associated with an oscilloscope is applied to detect the transmission signals. The driving CW laser (1064nm), together with signal generator and EO modulator are used to provide the modulation signal. The fiber connected to the driving CW laser is directly located above the photothermal absorber.

IV. Characterization

The transmission response of the fabricated device is shown in Fig. 3(a). One can see that a resonant peak of the

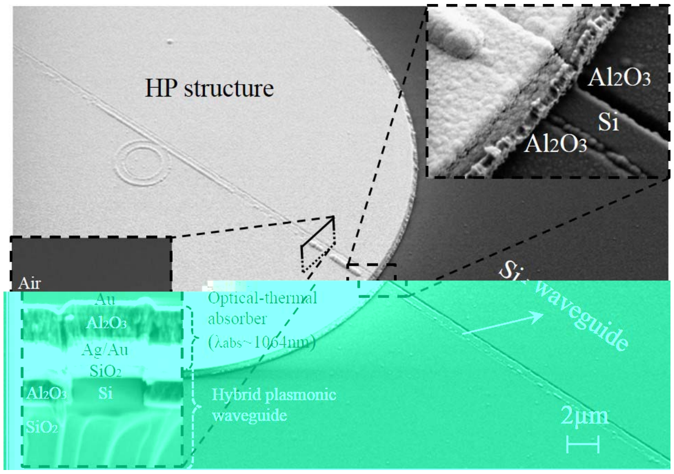

Fig. 2. Scanning electron microscope (SEM) images of HP donut resonator with photothermal plasmonic absorber. The upper right inset shows the coupling area between Si bus waveguide to HP waveguide. The lower left inset is the cross-section view of the fabricated device.

HP donut resonator is located at about 1564nm, with an extinction ratio (ER) of about 20dB. The loaded Q factor is around 600, which indicates that the initial Q factor of such a HP donut resonator should be larger than 1000, without the coupling loss between the bus waveguide and the resonator. This Q value is comparable to other types of HP disk/ring resonators, both from theoretical and experimental investigations

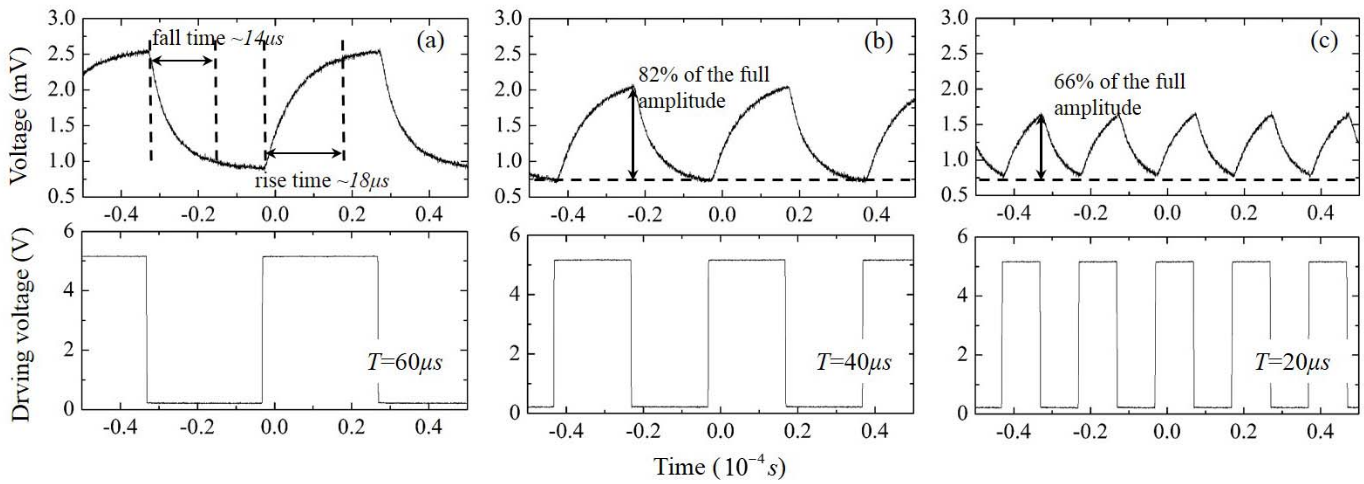

Fig. 4. Dynamic measurement results with (a) 60μs, (b) 40μs and (c) 20μs signal periods.

a ring resonator is 1.8μm with a loaded Q factor of about 600 at communication wavelengths, and the ER is larger than 20dB as seen from the static measurements. The photothermal absorber can absorb as much as 75% of optical power from a driving CW laser with 1064nm wavelength. The absorbed optical power can efficiently heat the HP donut resonator underneath, and hence change the resonant wavelength by Si thermal expansion effect. By applying 10mW of optical driving power, the output power at the resonant wavelength can increase 15dB with 18μs and 14μs rise and fall time, respectively. The fabricated HP device has a much smaller size as well as several times lower power consumption than pure SOI-based electrical-thermal components and can be used as an all-optical switch or low-speed modulator.

REFERENCES

[1] D. Dai and S. He, "A silicon-based hybrid plasmonic waveguide with a metal cap for a nano-scale light confinement," *Opt. Exp.*, vol. 17, no. 19, pp. 16646–16653, 2009.

[2] F. Lou, Z. Wang, D. Dai, L. Thylén, and L. Wosinski, "Experimental demonstration of ultra-compact directional couplers based on silicon hybrid plasmonic waveguides," *Appl. Phys. Lett.*, vol. 100, no. 24, p. 241105, 2012.

[3] A. Melikyan *et al.*, "High-speed plasmonic phase modulators," *Nature Photon.*, vol. 8, no. 3, pp. 229–233, 2014.

[4] R. F. Oulton, V. J. Sorger, D. A. Genov, D. F. P. Pile, and X. Zhang, "A hybrid plasmonic waveguide for subwavelength confinement and long-range propagation," *Nature Photon.*, vol. 2, no. 8, pp. 496–500, 2008.

[5] G. Li *et al.*, "25 Gb/s 1 V-driving CMOS ring modulator with integrated thermal tuning," *Opt. Exp.*, vol. 19, no. 21, pp. 20435–20443, 2011.

[6] F. Lou, D. Dai, L. Thylén, and L. Wosinski, "Design and analysis of ultra-compact EO polymer modulators based on hybrid plasmonic microring resonators," *Opt. Exp.*, vol. 21, no. 17, pp. 20041–20051, 2013.

[7] Z. Wang *et al.*, "Room-temperature InP distributed feedback laser array directly grown on silicon," *Nature Photon.*, vol. 9, no. 12, pp. 837–842, 2015.

[8] X. Sun, D. Dai, L. Thylén, and L. Wosinski, "High-sensitivity liquid refractive-index sensor based on a Mach–Zehnder interferometer with a double-slot hybrid plasmonic waveguide," *Opt. Exp.*, vol. 23, no. 20, pp. 25688–25699, 2015.

[9] F. Lou, L. Thylén, and L. Wosinski, "Ultra-sharp bends based on hybrid plasmonic waveguides," in *Proc. Eur. Conf. Opt. Commun. (ECOC)*, Sep. 2014, pp. 1–3.

[10] F. Lou, Z. Wang, D. Dai, L. Wosinski, and L. Thylén, "A sub-wavelength microdisk resonator based on hybrid plasmonic waveguides," in *Proc. Int. Photon. Optoelectron. Meetings (POEM)*, 2012, p. IF2A.5.

[11] J. Wang *et al.*, "Sub-μm^2 power splitters by using silicon hybrid plasmonic waveguides," *Opt. Exp.*, vol. 19, no. 2, pp. 838–847, 2011.

[12] X. Guan, H. Wu, Y. Shi, L. Wosinski, and D. Dai, "Ultracompact and broadband polarization beam splitter utilizing the evanescent coupling between a hybrid plasmonic waveguide and a silicon nanowire," *Opt. Lett.*, vol. 38, no. 16, pp. 3005–3008, 2013.

[13] F. Lou, D. Dai, and L. Wosinski, "Ultracompact polarization beam splitter based on a dielectric–hybrid plasmonic–dielectric coupler," *Opt. Lett.*, vol. 37, no. 16, pp. 3372–3374, 2012.

[14] X. Sun, D. Dai, L. Thylén, and L. Wosinski, "Double-slot hybrid plasmonic ring resonator used for optical sensors and modulators," *Photonics*, vol. 2, no. 4, pp. 1116–1130, 2015.

[15] D. Dai, Y. Shi, S. He, L. Wosinski, and L. Thylén, "Silicon hybrid plasmonic submicron-donut resonator with pure dielectric access waveguides," *Opt. Exp.*, vol. 19, no. 24, pp. 23671–23682, 2011.

[16] M. Yan, "Metal–insulator–metal light absorber: A continuous structure," *J. Opt.*, vol. 15, no. 2, p. 025006, 2013.

[17] X. Sun, L. Wosinski, and L. Thylén, "Nanoscale surface plasmon polariton disk resonators, a theoretical analysis," *IEEE J. Sel. Topics Quantum Electron.*, vol. 22, no. 2, Mar./Apr. 2016, Art. no. 4600106.

[18] X. Chen *et al.*, "Photothermally tunable silicon-microring-based optical add-drop filter through integrated light absorber," *Opt. Exp.*, vol. 22, no. 21, pp. 25233–25241, 2014.

[19] A. Densmore *et al.*, "Compact and low power thermo-optic switch using folded silicon waveguides," *Opt. Exp.*, vol. 17, no. 13, pp. 10457–10465, 2009.

[20] Y. Shi *et al.*, "All-optical switching of silicon disk resonator based on photothermal effect in metal–insulator–metal absorber," *Opt. Lett.*, vol. 39, no. 15, pp. 4431–4434, 2014.

[21] Y. Tang, Z. Wang, L. Wosinski, U. Westergren, and S. He, "Highly efficient nonuniform grating coupler for silicon-on-insulator nanophotonic circuits," *Opt. Lett.*, vol. 35, no. 8, pp. 1290–1292, 2010.

[22] Y. Song, J. Wang, Q. Li, M. Yan, and M. Qiu, "Broadband coupler between silicon waveguide and hybrid plasmonic waveguide," *Opt. Exp.*, vol. 18, no. 12, pp. 13173–13179, 2010.